1996A&A...309..521H

Astron. Astrophys. 309, 521–529 (1996)

ASTRONOMY AND ASTROPHYSICS

Spectroscopic orbit of the triple star 55 Ursae Majoris*

J. Horn, J. Kubát, P. Harmanec, P. Koubský, P. Hadrava, V. Šimon, S. Štefl, and P. Škoda**

Astronomický ústav, Akademie věd České republiky, 251 65 Ondřejov, Czech Republic

Received 29 May 1995 / Accepted 12 October 1995

Abstract. The first investigation of the known triple system 55 UMa ($2^d.55$ binary in a $\sim$ 1870-d orbit with the third star) based on electronic spectra led to several new findings about the system: (1) Discovery of spectral lines of the tertiary and an unambiguous detection of the lines of the secondary. Spectra of both primary and tertiary are of the same strength and correspond to spectral class A0V. The secondary spectrum is about twice fainter in the visual region and belongs probably also to spectral class A. (2) First self-consistent orbital solution describing close and wide orbit and the detection of apsidal motion for the close pair. The orbital period of the close pair was improved to ($2^d.5538380 \pm 0^d.0000046$) and basic physical elements for all three stars and the system were estimated. The orbital solution also gives the period of apsidal motion of the close pair of (450 $\pm$ 60) yr and leads to a good agreement with the published speckle-interferometric orbit for the distant companion if the longitude of periastron passage is increased by 180°.

Key words: stars: binaries: spectroscopic – stars: individual: 55 UMa – stars: fundamental parameters

1. Introduction

55 UMa (HD 98353, HR 4380, BD+38°2225; $V=4^m.78$) was reported to be a spectroscopic binary by Lee (1908). His observations were only published much later, by Frost et al. (1929). Lee measured lines of both components on three occasions. Henroteau (1919) also found, and was able to measure, the lines of both components. He derived the first orbital elements: $P=2^d.5$, K_1 = 38.5 km s^{-1}, K_2=54.5 km s^{-1}, e=0.11, ω_1=173°.4, γ=-3 km s^{-1}; the mass ratio M_2/M_1 being 0.706.

Only several decades later, Lloyd (1981) obtained a new orbital solution based on the Dominion Astrophysical Observatory spectrograms from 1954 to 1964. Using dispersions of 11 and 15 Å/mm he obtained a much higher semiamplitude (K_1 = 80.4 $\pm$ 2.0 km s^{-1}) and eccentricity (e=0.43 $\pm$ 0.03). He also improved the value of the orbital period to $2^d.55385 \pm 0^d.00002$. He measured the RVs of the secondary star on a few spectra only (without publishing them) and estimated the mass ratio to be about 0.9. Lloyd also scanned two plates and concluded that the spectral classes of both stars are between A5 and A9. He pointed out that available photometry indicated a spectral class A2 and suggested that at least one of the stars has a UV excess. We note, however, that several independent spectral classifications of 55 UMa quoted by Jaschek et al. (1964) and in the Strasbourg computerized bibliography agree on spectral type A2.

Several authors include 55 UMa among λ Boo stars (for an overview of the λ Boo phenomenon see Stürenburg 1993) or candidates (Hauck 1986, Renson et al. 1990, Iliev & Barzova 1994). The classification of 55 UMa as a λ Boo star should be reconsidered since most of the investigators did not consider the multiplicity of 55 UMa . Recently, Andrillat et al. (1995) investigated infrared CCD spectra (7570–11000 Å; dispersion of 33 Å/mm) of a group of λ Boo stars, including 55 UMa. They assigned 55 UMa a spectral class A6 shell, obviously again without taking the composite character of its spectrum into account.

McAlister et al. (1989) discovered a distant third companion to 55 UMa at 0".068 during their speckle-interferometric survey of bright stars. Further observations by McAlister et al. (1990, 1993) led to the determination of a complete orbit of 55 UMa C, with the following elements:

P = 1870^d.0, a = 0".089, ω = 45°.9, e=0.123,
$T_{\text{periastr.passage}}$ = JD 2446943 and i = 64°.4.

Jerzykiewicz (1974) did not find any significant light variations of 55 UMa related to the 2.55-d period.

We began to collect electronic spectra of 55 UMa with the Reticon in coudé spectrograph in Ondřejov and with the Aurélie spectrograph with a TH7832 detector at the Haute Provence Observatory. Combination of our new spectra with the previously published velocities allowed us to improve significantly

Send offprint requests to: J. Kubát

* This research is based on spectra from the Ondřejov and Haute Provence observatories. Table 1 is also available in electronic form at the CDS via anonymous ftp 130.79.128.5

** Dr. Jiří Horn died on December 13, 1994

© European Southern Observatory • Provided by the NASA Astrophysics Data System

1996A&A...309..521H

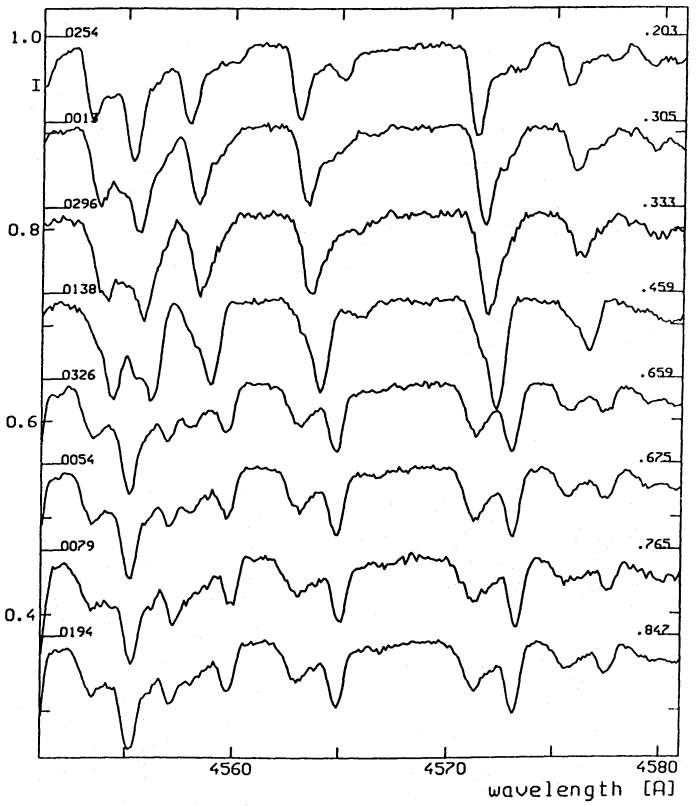

Fig. 1. A part of the blue Aurélie spectra of 55 UMa covering the spectral region 4541 – 4581 Å shown for several orbital phases. Unfortunately, only a limited interval of orbital phases was covered by these observations. Each spectrum is identified by the file number (cf. Table 1) and by orbital phase from periastron of the close orbit from solution 3 of Table 4.

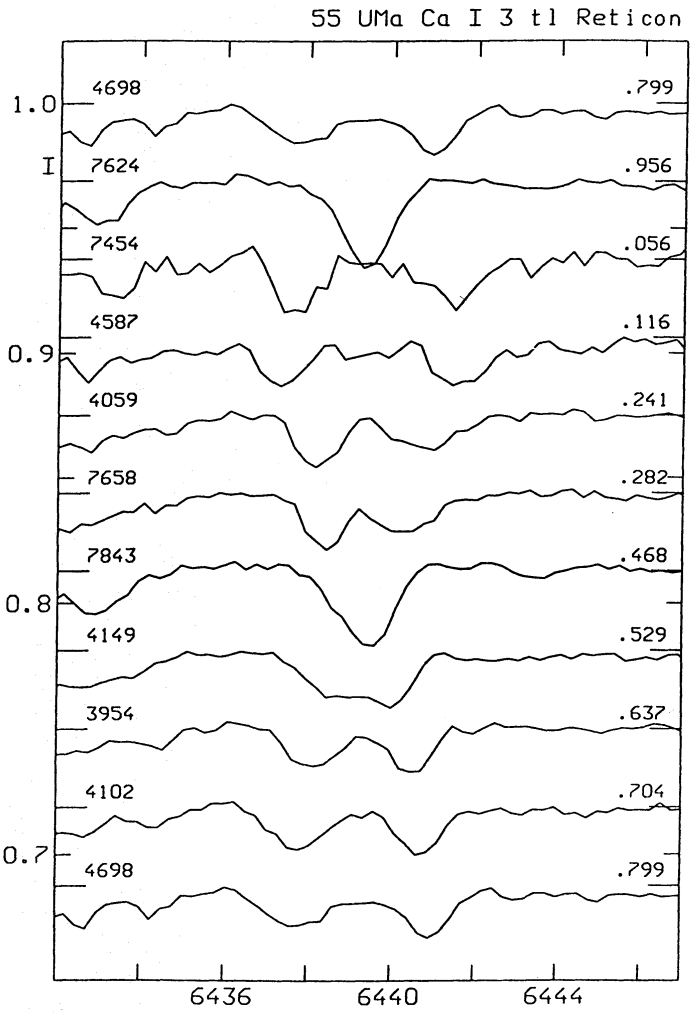

Fig. 2. Reticon spectra of 55 UMa in the neighbourhood of the Ca I line at 6439 Å. Each spectrum is identified by the file number (cf. Table 5) and by orbital phase from periastron of the close orbit from solution 3 of Table 4.

the knowledge of the basic physical elements of this interesting triple system and its components. Our results are described below.

2. Observations

2.1. New electronic spectra

Our own observations consist of the following two data sets:

1. 12 Aurélie spectra (dispersion 8.5 Å/mm) obtained by PK at the Haute Provence Observatory and covering three wavelength regions: 4430–4650, 6490–6700 Å, and 6530–6735 Å. For a detailed description of the Aurélie spectrograph, see Gillet et al. (1994).
2. 33 Reticon spectrograms obtained in the coudé focus of the Ondřejov 2.0-m telescope between February 1994 and April 1995. One spectrogram has a dispersion of 8.5 Å/mm and covers the spectral region 4740–4960 Å. The remaining ones have a linear dispersion of 17.1 Å/mm and cover a wavelength region of about 400 Å centered partly on 6500 Å, and partly on about 6200 Å.

The reduction of all electronic spectra was carried out using the Pascal program SPEFO, developed by JH.

2.2. Radial velocities from the electronic spectra

Figs. 1 and 2 show selected parts of the electronic spectra of 55 UMa in the blue and red spectral regions, respectively, for various orbital phases. Already their first inspection and preliminary RV measurements revealed that the spectra are more complicated than what one would expect from the previous descriptions. Lloyd (1981) claimed that the components were never completely resolved. However, the electronic spectra reveal two, and sometimes three distinct components, depending on the particular orbital phase. In the spectra obtained at elongations of the close pair some lines of the distant third component are clearly visible. Most of the lines of the third star are almost as strong as the lines of the primary while the lines of the secondary are weaker and broader. This is well seen, e.g., for the Si II 2 doublet at 6347 and 6371 Å (see Fig. 3).

Using the program SPEFO (which permits settings on line centres on the computer screen using direct and reverse images of the line profile) we measured primary, secondary and – whenever possible – tertiary RVs. All RVs from the spectra

© European Southern Observatory • Provided by the NASA Astrophysics Data System

1996A&A...309..521H

Table 1. OHP and Ondřejov radial velocities of 55 UMa.

File	HJD (JD-2400000)	RV_1 (all) (km s^{-1})	w_1	RV_1 (Ca I) (km s^{-1})	w_1	RV_2 (Ca I) (km s^{-1})	w_2	λ range (Å/mm)
AUR40280	49371.6577	56.3	0.705	–	–	–	–	6490–6700
AUR40455	49374.6718	57.9	0.705	–	–	–	–	6490–6700
AUR50013	49475.4238	-28.2	2.350	-25.9	0.235	36.8	0.235	4433–4647
AUR50054	49476.3676	63.0	2.350	58.0	0.235	-51.1	0.235	4433–4647
AUR50079	49476.5979	74.6	2.350	72.9	0.470	-60.7	0.470	4433–4647
AUR50138	49478.3702	10.9	2.350	13.5	0.470	–	–	4433–4647
AUR50194	49479.3621	67.7	2.350	66.7	0.470	-49.6	0.470	4433–4647
AUR50254	49480.3412	-52.1	2.350	-52.9	0.470	66.1	0.470	4433–4647
AUR50268	49480.3936	-43.4	0.235	–	–	–	–	6530–6735
AUR50296	49480.6033	-16.2	2.350	-9.6	0.235	36.4	0.235	4433–4647
AUR50321	49481.3677	54.4	2.350	–	–	–	–	4433–4647
AUR50326	49481.4367	60.7	2.350	61.0	0.470	-45.7	0.470	4433–4647
RET3870	49408.4646	-75.9	0.819	-88.7	0.117	107.1	0.234	6297–6731
RET3886	49416.4897	-51.4	2.350	–	–	–	–	4743–4957
RET3935	49421.3479	-82.1	0.819	-84.5	0.117	110.2	0.234	6297–6731
RET3942	49422.3674	26.9	0.819	31.8	0.234	-25.7	0.234	6297–6731
RET3954	49422.6425	56.1	0.819	56.8	0.234	-52.9	0.234	6297–6731
RET4039	49438.3720	58.8	0.702	70.9	0.234	-65.9	0.117	6297–6731
RET4059	49439.5070	-49.1	1.053	-52.1	0.234	66.0	0.234	6297–6731
RET4102	49448.3515	66.5	0.819	66.2	0.234	-68.3	0.234	6298–6731
RET4149	49450.4573	24.0	0.702	29.7	0.234	-38.6	0.234	6298–6731
RET4300	49464.4056	-25.5	1.170	-31.9	0.234	44.1	0.234	6296–6730
RET4562	49471.3573	64.8	0.819	67.0	0.234	-59.2	0.234	6297–6730
RET4587	49472.3867	-83.9	0.819	-88.3	0.117	108.8	0.117	6298–6731
RET4698	49484.3460	73.4	0.936	70.7	0.234	-64.4	0.234	6297–6731
RET4722	49486.3980	40.9	0.702	41.0	0.234	-53.9	0.234	6296–6729
RET7435	49734.6648	68.2	0.702	71.3	0.234	-73.9	0.117	6301–6735
RET7454	49745.4939	-71.6	0.468	-72.0	0.117	93.6	0.234	6301–6735
RET7579	49770.2846	63.6	0.819	64.4	0.234	-77.7	0.234	6306–6740
RET7593	49771.5379	-47.9	0.702	-51.9	0.234	65.5	0.234	6306–6740
RET7624	49778.4439	1.3	1.170	3.3	0.234	3.3	0.234	6306–6739
RET7658	49784.3794	-38.5	0.936	-40.8	0.234	43.3	0.234	6305–6739
RET7666	49784.4841	-23.4	0.702	-24.0	0.234	33.0	0.234	5937–6371
RET7700	49785.4169	58.6	1.170	64.3	0.234	-61.9	0.351	5943–6377
RET7702	49785.4881	62.7	1.053	65.9	0.351	-72.7	0.234	5943–6377
RET7714	49787.4925	9.3	0.936	12.2	0.351	-26.6	0.351	5964–6398
RET7738	49788.5120	39.1	0.819	43.1	0.351	-47.8	0.351	5969–6402
RET7800	49801.3492	16.5	0.936	20.4	0.351	-36.5	0.351	5971–6405
RET7807	49801.4213	0.6	1.170	1.4	0.351	1.4	0.351	5971–6405
RET7811	49801.5053	-21.1	0.702	-17.9	0.234	18.7	0.234	5971–6405
RET7814	49801.5817	-52.0	0.936	-53.6	0.351	65.8	0.234	5971–6405
RET7843	49810.3919	4.8	1.170	8.4	0.702	-35.0	0.468	6053–6487
RET7845	49810.4752	7.9	1.170	13.6	0.702	-37.6	0.585	6053–6487
RET7868	49811.3492	64.3	1.170	67.3	0.468	-74.6	0.351	5967–6400
RET7870	49811.4065	58.2	1.170	59.9	0.351	-64.4	0.234	5967–6400

Notes: Symbols AUR and RET in the column "File" denote electronic spectra from the Haute Provence Aurélie spectrograph and from the Ondřejov coudé spectrograph with the Reticon, respectively. RV_1 and RV_2 denote the mean radial velocities of the primary and secondary, respectively; 'all' indicates the mean RV of all lines, Ca I denotes the mean RVs of the lines of neutral calcium only; w_1 and w_2 are the corresponding weights, assigned according to formula 1. The last column indicates the wavelength range covered by the spectra.

© European Southern Observatory • Provided by the NASA Astrophysics Data System

1996A&A...309..521H

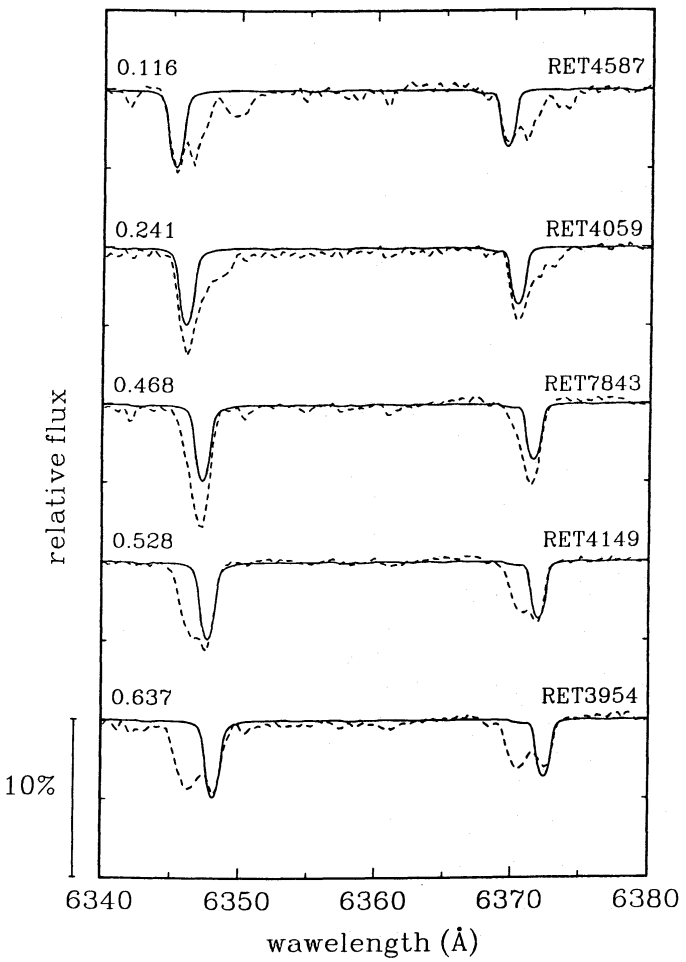

Fig. 3. A comparison of the theoretical spectrum of the primary with the observed spectra of Si II 2 lines at several orbital phases. The arrows with numbers indicate the corresponding star (1 – primary, 2 – secondary, 3 – tertiary).

covering the red parts of the optical spectrum were corrected via the measurements of telluric lines as discussed in Appendix. We therefore treated the RVs from the red Reticon *and* Aurélie spectra as having one common RV zero point (denoted by suffix *I* in Tables 3 and 4). This was not possible for the blue Aurélie spectra. Since no IAU RV standards were observed along with these spectra, the RVs from them were treated as having a different zero point in all orbital solutions (see below) which is denoted by suffix *H* in Tables 3 and 4.

It quickly turned out that while the lines of the primary can usually be measured reliably, this is not so for the lines of the secondary which are weak and often blended with the lines of the tertiary. Consequently, the corresponding measurements of radial velocities do not yield reliable values. This can be illustrated by means of the Si II 6347 and 6371 lines. We measured equivalent widths for these lines at various orbital phases and did not find any change of the *total* equivalent width of the superposition of all three components. This indicates that the apparent spectral variations are solely due to blending of three spectra and their mutual shifts in wavelength and that no significant line strength variations are present. In order to make reliable identification of the lines of all three components we decided to fit the spectra of individual stars with the help of theoretical synthetic spectra. We used a new grid of LTE line blanketed plane-parallel model atmospheres of Kurucz (1993). Synthetic spectra were calculated with the computer code SYNSPEC (developed by I.Hubeny – for a recent description see Hubeny et al. 1994). We found that the model with $T_{\rm eff}$= 9500 K and log g = 4.5 [CGS] fits the spectrum of the primary quite well. The best fit was obtained for the rotational velocity of 33 km s^{-1}. The spectra of the primary and tertiary are very similar in the observed spectral regions. Consequently, we adopted the same fit for the tertiary as for the primary. Corresponding rotational velocity of the tertiary is 55 km s^{-1}, however. On the other hand, any fit of the spectrum of the secondary is very uncertain, basically due to the relative weakness of its spectrum, and all we can say at the moment is that the secondary is of a spectral class A. The fit of the primary lines of Si II 6347 Å and 6371 Å is shown in Fig. 3. Notice the presence of *three* resolved components of these lines in the uppermost spectrum. Starting from the left, the components belong to the primary, tertiary, and secondary stars. On all other spectrograms the lines of the tertiary are blended either with those of primary or secondary, making a more detailed analysis difficult.

Fortunately, it turned out that the tertiary has no detectable lines of Ca I, while just these lines are quite strong and well resolved for both primary and secondary. This makes the Ca I lines well suited for the radial-velocity measurements of the secondary. The results of the RV measurements are collected in Table 1.

2.3. *Compilation of published RVs of 55 UMa*

Through a search in the astronomical literature and databases, we were able to find 184 radial velocities (RVs hereafter) from 6 different observatories (see Table 2).

All observations were weighted according to the formula

$$w = Q \cdot N \cdot D^{-1} \qquad (1)$$

where N is the number of measured lines forming the spectrum mean RV (we used N = 10 for actual N > 10 in order not to overestimate an effect of a single spectrogram), and D is the linear dispersion of the spectrogram (in Å/mm). To take into account the much better definition of line profiles from electronic spectra (due to their low noise), we introduced an ad hoc parameter Q, and put Q = 1 for photographic, and Q = 2 for electronic spectra. Our choice of inverse proportionality between the weight and linear dispersion D needs some clarification. The weight should be inversely proportional to the square of the mean external error for a constant star measured with a given instrument. A detailed study of 33 Å/mm and 66 Å/mm David Dunlap spectra by Crampton et al. (1967) shows that the ratio of the squares of external errors between the two spectrographs is indeed close to 2 for all investigated groups of stars. We therefore believe that our weighting method is a reasonable approach. Moreover, we have verified that the results are not critically sensitive to the use of the weights.

© European Southern Observatory • Provided by the NASA Astrophysics Data System

1996A&A...309..521H

Because of the heterogeneity of the material used, the following comments about the selection of the final data set are relevant:

File A The number of actually measured lines is not given in the original paper but it is clear that it was rather high. We therefore adopted $N = 10$ and the mean prismatic dispersions which resulted in $w = 0.333$ for single-prism, and $w = 0.5$ for double-prism spectra. In cases when two measurements for the same plate are tabulated we used the arithmetic mean RV from the two measurements.

File B Weights proportional to the number of measured lines and their quality (on a scale from 1 to 3) are tabulated in the original source. We simply divided these original weights by the mean dispersion of the instrument (40 Å/mm) to obtain weights on our scale. Since quality 2 refers to an average line, all weights larger than 0.5 were set equal to 0.5. All mean RVs were increased by +2.0 km s^{-1} to correct them into the GCVS velocity system (see Table 3 in Beardsley 1969). We found that the Julian dates starting with the plates obtained on 1916 April 28 till the end of the data file, quoted in the original paper, are incorrect and have to be increased by 1 day.

File C We use again the mean RV in one case when two separate measurements of the same plate are given.

File D Neither dispersion nor the number of measured lines is known; only rms errors of the mean RVs are tabulated. We adopt weight of 0.5 for the first two, and 0.25 for the remaining three RVs.

File E Weights quoted in the original paper were divided by the spectrograph dispersion to derive weights. For resulting weights larger than 0.263, we set w=0.263.

File G Two different dispersions, 11 and 15 Å/mm, were alternately used and about 20 lines measured. Since no details are given, we adopt $D = 13$ and $N = 10$, thus $w = 0.769$, for all spectra.

3. Period analysis and orbital solution

Since the periodicity of the closer orbit seems to be well established, we only carried out a period search in the neighbourhood of the 2.554-d period to check for possible secular changes. To this end, we used the phase dispersion minimization technique (Stellingwerf 1978), and analyzed separately the old and new RVs of the primary (files A through F, and G to I, respectively). To take the nonsinusoidal character of the RV curve into account, the minimum RV dispersion was searched using 7 bins in phase in three different representations. Corresponding periodograms are shown in Fig. 4. It is seen that the aliasing problem is quite acute with the new data. Yet, the best periods detected in both data sets, $2^d.553806$ and $2^d.553802$, respectively, are nearly identical.

As the next step, we calculated formal orbital solutions, again separately for the old and new primary RVs. (All orbital solutions presented here have been calculated using program FOTEL: Hadrava 1990, 1992.) The corresponding RV curves are shown in Fig. 5. It is seen that the old RVs follow a RV curve in phase with the new RVs of the primary *but with a strongly reduced amplitude*. This is clearly due to a heavy blending of spectral lines from all three stars which is inevitable for lower-dispersion and lower-resolution spectra. The lines of the primary blend with the comparably strong lines of the tertiary (the latter varying only a little in RV). This explains the observed reduced RV amplitude of the primary in all old spectrograms. This fact has an unpleasant consequence: The old RVs cannot be combined with the new ones for any improvement of the value of the 2.55-d period since the overlapping RV variations due to motion in close and wide orbits and due to an apsidal motion of the close pair (see below) could not be treated consistently in the combined set. One can only conclude that the 2.5538-d period has not changed significantly between the old and new data: The corresponding values from the formal orbital solutions are ($2^d.553817 \pm 0^d.000063$) and ($2^d.5537986 \pm 0^d.0000041$), respectively. An alternative explanation of the difference in RV amplitude between old and new data – namely a precession of the close orbit with real changes of the velocity amplitudes observed – seems rather unlikely since it would imply a very short period of precession. Precession in a triple system with non-coplanar orbits (like 55 UMa – see below) was indeed found for the eclipsing binary IU Aur – see Mayer and Drechsel (1987), Drechsel et al. (1994).

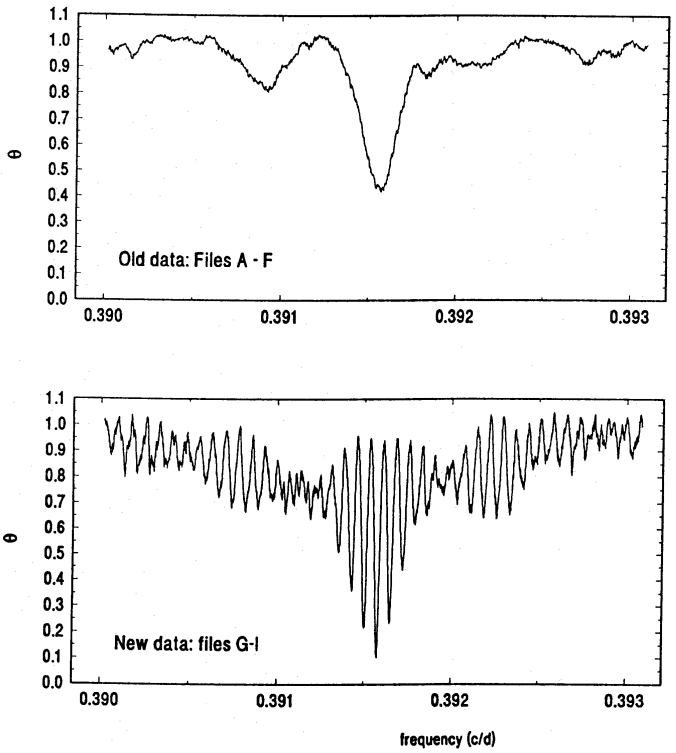

Fig. 4. PDM periodograms for the old and new RVs of 55 UMa in the neighbourhood of the $2^d.554$ period.

Further analysis was, therefore, limited to only Lloyd's and our new data (i.e. files G - I).

We first compared the orbital solutions for the RVs of the primary calculated separately for Lloyd's and for our data (see solutions 1 and 2 of Table 3). It is immediately seen that the elements from both data sets differ quite significantly, especially in

© European Southern Observatory • Provided by the NASA Astrophysics Data System

1996A&A...309..521H

Table 2. The radial-velocity observations of 55 UMa

File	Source	Epoch (JD-2400000)	No. of RVs prim./sec.	Disp. Å/mm
A	Frost et al. (1929)	17632–22448	11/ 2	30+20
B	Beardsley (1969)	18303–20993	111/ 0	40
C	Campbell & Moore (1928)	18690–18779	3/ 0	11
D	Abt (1970)	19826–20967	5/ 0	?
E	Henroteau (1923)	20955–21306	10/ 0	38
F	Harper (1937)	23473–23523	3/ 0	30
G	Lloyd (1981)	34831–37740	41/ 0	11+15
H	OHP Aurélie	49371–49481	12/11	8.5
I	Ondřejov Reticon	49408–49811	33/33	17

Notes: Telescope and instruments corresponding to individual data files: A... Yerkes 1.02-m refractor, 1- and 2-prism spgs.; B... Allegheny 0.79-m Keeler Memorial reflector, 1-prism Mellon spg.; C... Lick 0.90-m reflector; new Mills 3-prism spg.; D... Mt.Wilson 1.5-m reflector; prism. spg.; E... Ann Arbor 0.95-m reflector; 2-prism spg.; F... Dominion Astrophysical Observatory, 1.83-m reflector, prism spg. with medium-focus IM camera; G... Dominion Astrophysical Observatory, 1.83-m reflector, prism spg. with IIL and IIM cameras; H... Haute Provence Observatory, Aurélie coudé grating spectrograph with a TH7832 detector; I... Ondřejov 2.0-m reflector, coudé grating spectrograph, Reticon RL 1872F/30 detector.

Table 3. Comparison of the *close binary* solutions for Lloyd's and new radial-velocity observations of 55 UMa

element	solution 1 by Lloyd	solution 1 by us	solution 2 files H-I
P (d)	2.55385	2.553823	2.553902
rms error	0.00002	0.000022	0.000083
$T_{periastr.}$	34830.88	34830.926	49602.286
rms error	0.02	0.026	0.017
$T_{prim.ecl.}$	–	34830.942	49602.236
$T_{min.RV}$	–	34831.293	49602.609
K (km s^{-1})	80.4 ± 2.0	77.7 ± 1.8	72.8 ± 1.2
e	0.43 ± 0.03	0.41 ± 0.02	0.30 ± 0.01
ω (deg.)	74.3 ± 3.0	80.3 ± 3.2	103.6 ± 2.7
γ_G (km s^{-1})	-4.6 ± 1.2	-5.5 ± 1.1	–
γ_H (km s^{-1})	–	–	6.8 ± 0.9
γ_I (km s^{-1})	–	–	0.4 ± 0.9
No. of RVs	41	41	45
rms (km s^{-1})	–	6.47	3.72

Notes: Row "rms" contains the root-mean-square error of one observation of unit weight. The suffixes of individual γ velocities corresponds to data set files in Table 2 (see also the remarks on individual data files in subsection 2.3). However, suffix *H* denotes RVs from blue Aurélie spectra while suffix *I* refers to the red Aurélie *and* Reticon spectra corrected to the same RV zero point. All epochs are in HJD-2400000. The small differences in the original Lloyd's solution and our re-calculation result probably from our use of the weights. Note, however, that the differences are within the errors of respective elements.

Table 4. *Triple-star* orbital solutions for 55 UMa

element	solution 3 all lines files G-I	solution 4 Ca I lines files H-I
CLOSE ORBIT		
$P_{anomalistic}$ (d)	2.5538380	2.5538380
rms error	0.0000046	fixed
P (d)	2.5537985	2.5537985 fixed
$\dot{\omega}$ (deg. yr^{-1})	0.80 ± 0.11	0.80 fixed
$T_{periastr.}$	49602.337	49602.367
rms error	0.014	0.016
$T_{prim.ecl.}$	49602.260	49602.266
$T_{min.RV}$	49602.588	49602.594
K_1 (km s^{-1})	75.8 ± 1.1	78.8 ± 1.8
K_2 (km s^{-1})	86.6 ± 1.8	87.8 ± 2.4
e	0.336 ± 0.010	0.329 ± 0.013
ω (deg.)	112.8 ± 2.4	119.1 ± 2.7
WIDE ORBIT		
P (d)	1870.0 fixed	1870.0 fixed
$T_{periastr.}$	46943.0 fixed	46943.0 fixed
$T_{min.RV}$	48551.6 fixed	48551.6 fixed
K_{1-2} (km s^{-1})	7.7 ± 1.5	8.0 ± 1.5
e	0.123 fixed	0.123 fixed
ω (deg.)	242.3 ± 9.9	242.3 fixed
γ_G (km s^{-1})	-5.3 ± 1.0	–
γ_H (km s^{-1})	0.1 ± 1.9	0.9 ± 1.5
γ_I (km s^{-1})	-3.8 ± 1.6	-3.7 ± 0.9
No. of RVs	125	79
rms (km s^{-1})	5.33	6.04

Notes: see Notes under the Table 3

the longitude of periastron, eccentricity and in systemic velocity. A possible explanation is that there is a measurable apsidal motion and that the close binary also moves in orbit with the third body discovered by interferometry, lines of which are clearly visible in some of our spectra. Note that while Lloyd's data span over one and a half of the 1870-d period of the wide orbit, the new data cover only slightly more than 400 d. We therefore calculated another orbital solution, allowing for the periastron advance and taking the third body into account. In doing so, we kept the orbital period, eccentricity and the epoch of the periastron passage of the third body fixed at values found by McAlister et al. (1993) from the interferometric data and solved for the longitude of periastron and semi-amplitude of the orbital motion of the wide orbit. This solution 3 is presented in Table 4. It indicates that the orbital motion of the wide system is indeed

© European Southern Observatory • Provided by the NASA Astrophysics Data System

1996A&A...309..521H

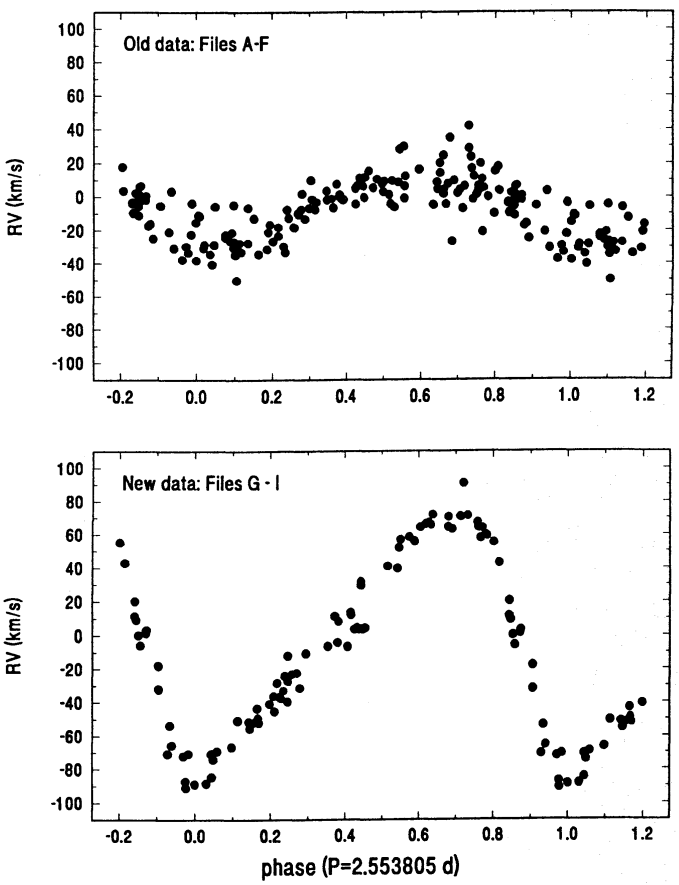

Fig. 5. RV curves based on the old and new observations of 55 UMa plotted versus phase of the $2\overset{d}{.}55383$ period (with respect to an arbitrary epoch).

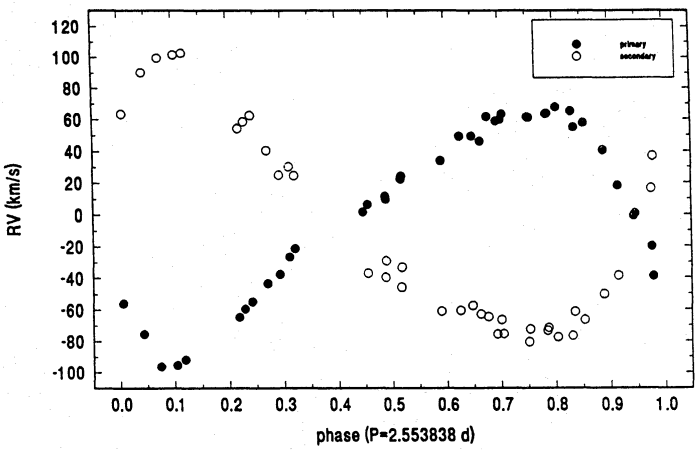

Fig. 6. RV curves of the primary and secondary of 55 UMa based on measurements of Ca I lines in our spectra. Phases are calculated from periastron (solution 4 of Table 4)

affecting the measured RVs. At the same time, we found that the value of the longitude of the periastron published by McAlister et al. has to be increased by 180° (such an ambiguity is inherent to speckle-interferometric data).

4. Basic physical elements of the triple system

Since Lloyd (1981) published only mean RVs of all lines, it was deemed necessary to adopt the mean RVs also for the electronic spectra in solution 3. Obviously, solution 3 thus provides the highest currently achievable accuracy in the determination of the value of 2.554-d period and of the rate of apsidal motion. However, this does not seem optimal for the determination of the physical elements of the triple system and its component stars. To this end, we fixed all parameters of the wide orbit and the value of the periastron advance at the values of solution 3 and calculated yet another solution (solution 4 – see Table 4 and Fig. 6) based on RVs of the Ca I lines only measured solely in the electronic spectra. These lines seem optimal for the given purpose since the Ca I lines of the primary and secondary are best resolved while the Ca I lines of the tertiary are below the detection threshold - cf. Fig. 2.

In principle, our results now provide a rather definitive orbital solution for the close pair but a preliminary one for the wide orbit. Keeping this limitation in mind, it is interesting to see how consistent our results are in terms of stellar masses, radii and other basic physical elements. The radiative parameters for the primary which we derived from the model fits of the blue and red spectra (see above) closely correspond to the spectral type A0V. We therefore adopted the mass and radius of the primary from Harmanec's (1988) mass and radius vs. $T_{\rm eff}$ relations based on modern binary data

$$M_1 = (2.26 \pm 0.23) M_\odot \quad \text{and} \quad R_1 = (2.1 \pm 0.1) R_\odot$$

which – in combination with solution 4 – implies

$$i_{1-2} = (38 \pm 7)^\circ \quad \text{and} \quad M_2 = (2.0 \pm 0.3) M_\odot$$

for the inclination of the close orbit and the mass of the secondary. The radius of the secondary corresponding to its mass should be

$$R_2 = (2.0 \pm 0.2) R_\odot .$$

According to the estimated radiative parameters, the mass and radius of the third star should be approximately the same as for the primary.

Harmanec (1988) showed that the rotation of the majority of well-observed binaries in eccentric orbits corresponds to synchronization in periastron. For the three components of 55 UMa we found the projected rotational velocities of 33, 50, and 55 km s^{-1}, respectively, with the relative error of 5%.

Solution 4 and synchronization in periastron would imply the rotational period of $1\overset{d}{.}2$ for components 1 and 2. This can be compared to the true rotational period of components 1 through 3, estimated from their V sin i, orbital inclination (assuming that rotational axes are perpendicular to the orbital plane) and radii: $2\overset{d}{.}0 \pm 0\overset{d}{.}6$, $1\overset{d}{.}2 \pm 0\overset{d}{.}4$, and $1\overset{d}{.}2 \pm 0\overset{d}{.}4$.

This is potentially a very interesting result (regardless the large relative errors) since it implies that the primary rotates about twice slower than it would correspond to its synchronization in periastron. This result is opposite to what was found for

© European Southern Observatory • Provided by the NASA Astrophysics Data System

1996A&A...309..521H

Spica (Smith 1985) and ε Per (Tarasov et al. 1995) for which the primaries rotate twice faster than synchronization in periastron would require.

Even more puzzling is the fact that the tertiary seems to have the same period of rotation as the secondary.

If we adopt the inclination of the wide orbit from the published (unfortunately no error estimates were quoted by the authors) interferometric solution,

$$i_{1\&2-3} = 64.4°,$$

solution 4 implies the mass of the tertiary component

$$M_3 = (1.7 \pm 1.1) M_\odot$$

for the total mass of the close pair of (4.3 ± 0.5) $M_\odot$ estimated above. Considering the large associated error, this mass does not contradict the estimated radiative parameters of the tertiary.

The semimajor axis of the wide orbit is (1160 ± 310) $R_\odot$. Compared to its angular value of $0''.089$, derived by McAlister et al. (1993), it implies an approximate distance of (61 ± 16) pc to the system. The observed V magnitude of the system is $4^m.79$ (Johnson et al. 1966), therefore M_V(total) = $0^m.88$. The estimated radii and effective temperatures of the components would imply a visual magnitude of the triple star of $-0^m.07$. This shows that our working model of the system is not fully consistent at the moment. At the same time, this exercise demonstrated that individual component masses of all three stars can be derived through continuing observations over the next 3–4 years which will define the RV curve of component 3 directly. Since the inclination of the wide orbit is known from interferometry, the sum of masses of the primary and secondary, and the mass of the tertiary would follow immediately from the orbital solution for the wide orbit. Using the mass ratio M_2/M_1 from our solution for the close orbit, one then also obtains the individual masses of the primary and secondary.

Finally, we note that solution 3 implies an apsidal period of (450 ± 60) yrs for the periastron advance of the close pair.

5. Conclusions

The first investigation of the triple system 55 UMa based on electronic spectra led to the following results:

1. Spectral lines of all three stars are present in the observed optical spectrum. For most ions, the spectral lines of the tertiary are almost as strong as the lines of the primary; the lines of the secondary are about twice fainter. All three stars are of spectral class A; the primary and tertiary seem to have a spectral class A0V. No evidence of phase-dependent line-strength variations was found. The classification of 55 UMa as a λ Boo star should be re-investigated in the light of the above findings.
2. The eccentricity of the close orbit is $e = 0.329 \pm 0.013$ which is lower than the value 0.43 of Lloyd (1981). The high eccentricity following from Lloyd's RVs only was obviously caused by the effect of varying systemic velocity of the close pair due to motion in the wide orbit which was not considered in original binary-star solutions. Our new value is clearly to be preferred since it was calculated for a triple star, includes the apsidal motion and is based on the lines of both primary and secondary stars. We also improved the corresponding period to a value of $2^d.5538380 \pm 0^d.0000046$.
3. Evidence for an apsidal motion of the close orbit, with a period of about 450 yrs, was found from the comparison of new RVs with those published by Lloyd (1981).
4. Preliminary estimate of the basic physical elements of the system and its individual components is presented. It was pointed out that accurate individual masses of all three stars can be derived after another 3-4 years of observations. Application of modern methods of spectrum disentangling (Hadrava 1995) appears desirable for future solutions.

Acknowledgements. We are grateful to the OHP and Ondřejov Observatory staff for their help during the observations. The installation of the Reticon RL-1872F/30 detector in the coudé focus of the Ondřejov 2-m telescope was made possible due to a generous loan of the detector and its control electronics from the Lick Observatory. Our special thanks for this belong to Professor Steven S. Vogt. The successful implementation of the Lick Reticon system was fostered by the enthusiastic and efficient effort of several highly skilled Ondřejov Observatory technicians: Messrs. K. Havlíček, K. Kalaš, J. Honsa, J. Vacek, and F. Žďárský. PK thanks the Observatoire de Paris for the hospitality and financial support during his visit which was also partly supported by the grant No.0025 of the Grant agency of the Czech Republic. Dr. Robert Kurucz kindly provided us with his set of CD-ROMs, while Dr. M. Jerzykiewicz kindly communicated the details of his photoelectric observations of 55 UMa. The use of the computerized bibliography from the Strasbourg Astronomical Data Centre is also gratefully acknowledged. Finally, the constructive criticism of an earlier version of the paper and a careful proofreading of the manuscript by the referee, Dr. Horst Drechsel, and by Dr. P. Mayer are greatly acknowledged.

Appendix A: investigation of the RV zero point of the Reticon RL-1872F/30 detector at Ondřejov observatory

The RV zero point of the Reticon detector was tested both by frequent observations of the IAU RV standards and by RV measurements of selected strong and unblended telluric lines. Of course, these telluric lines could only be measured for early-type stars but not for the late-type RV standards whose spectra are crowded with numerous stellar lines.

All initial reductions of the spectrograms were carried out with the Pascal program SPEFO developed by JH. In the first step of the investigation, we measured the set of telluric lines, listed in Table 5, in many spectra of various blue stars observed. It quickly turned out that the zero point of the Reticon in the Ondřejov coudé spectrograph can indeed vary for a few km s^{-1} from night to night. Typical rms errors of the mean RV of atmospheric lines of Table 5 range between 0.2 and 0.5 km s^{-1}. The time variation of the RV zero point was found to be slow and smooth and its value can, therefore, be safely interpolated for the red stars for which the atmospheric-line measurements cannot be carried out directly. The only discontinuities in the

© European Southern Observatory • Provided by the NASA Astrophysics Data System

1996A&A...309..521H

Table 5. A selection of telluric lines measured in the stellar spectra of early-type stars

Wavelength (Å)	Line	Wavelength (Å)	Line
6280.3950	atm O_2	6514.7280	atm H_2O
6281.1792	atm O_2	6516.593	atm H_2O 2x
6290.2222	atm O_2	6523.8442	atm H_2O
6297.2651	atm H_2O	6532.3540	atm H_2O
6298.4570	atm O_2	6534.000	atm H_2O
6299.2290	atm O_2	6543.9048	atm H_2O
6302.0000	atm O_2	6548.6221	atm H_2O
6302.7632	atm O_2	6552.6270	atm H_2O
6305.8101	atm O_2	6557.1729	atm H_2O
6306.5669	atm O_2	6572.0698	atm H_2O
6310.6372	atm O_2	6574.8491	atm H_2O
6490.7910	atm H_2O	6594.3701	atm H_2O
6495.8662	atm H_2O		

Table 6. Mean measured radial velocities of the IAU standards

Star	HD	RV (km s^{-1})	RV-RV_{IAU} (km s^{-1})	No.
α Cas	3712	-3.98 ± 0.16	-0.08	51
α Ari	12929	-13.58 ± 0.29	0.72	6
β Gem	62509	3.90 ± 0.60	0.60	2
α Boo	124897	-4.74 ± 0.30	0.56	30

Notes: The errors quoted with the mean RVs are the rms errors of the mean value. Column 'No.' contains the number of individual observations used to calculate the mean.

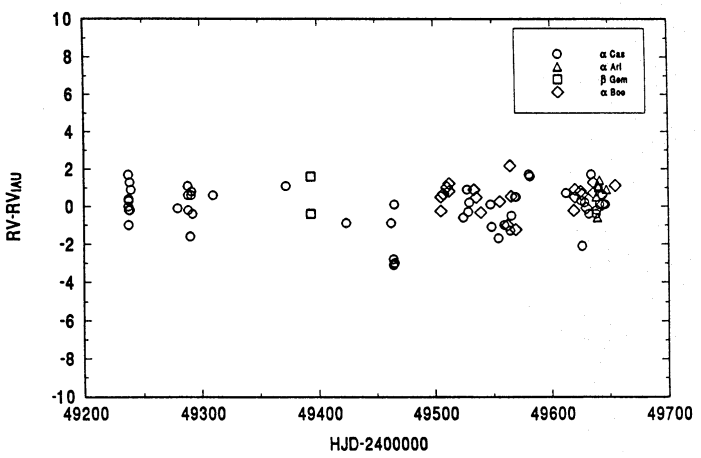

Fig. 7. Individual RVs of the IAU RV standards from the Ondřejov Reticon spectra.

zero-point change were noted on occasions when the vacuum of the detector dewar was renewed (typically every 3 months).

We measured a set of solar-spectrum lines in the spectra of several IAU RV standards. The wavelengths of measured stellar lines were taken from Moore (1945). Mean measured RV of each spectrum of the RV standards was corrected for the RV difference between the corresponding calculated heliocentric RV correction and the mean measured atmospheric-line RV for a blue star observed immediately prior or after the RV standard in question. The mean values of these corrected RV observations for several IAU standards are listed in Table 6. Individual observations are shown in Fig. 7 to give an estimate of the real instrumental accuracy of the individual RV measurements. The mean deviation of the Ondřejov values from the IAU standard ones, weighted by the number of measured spectra, is +0.20 km s^{-1}.

References

Abt H.A. 1970, ApJS 19, 387
Andrillat Y., Jaschek C., Jaschek M. 1995, A&A 299, 493
Beardsley W.R. 1969, Publ. Allegheny Obs. Univ. Pittsburg No. 7
Campbell W.W., Moore J.H. 1928, Publ. Lick Obs. 16, 1
Crampton D., Heard J.F., Hube D.P., Rice J.B. 1967, in Determination of Radial velocities and Their Applications, IAU Symp. 30, Ed. by A.H. Batten and J.F. Heard, Academic Press, London/New York, p.49
Drechsel H., Haas S., Lorenz R., Mayer P. 1994, A&A 284, 853
Frost E.B., Barrett S.B., Struve O. 1929, Publ. Yerkes Obs. 7, Part 1, 1
Gillet D., Burnage R., Kohler D., Lacroix D., Adrianzyk G., Baietto J.C., Berger J.P., Goillandeau M., Guillaume C., Joly C., Meunier J.P., Rimbaud G., Vin A. 1994, A&AS 108, 181
Hadrava P. 1990, Contr. Astron. Obs. Skalnaté Pleso 20, 23
Hadrava P. 1992, FOTEL: User's guide, release Nov. 13, 1992
Hadrava P. 1995, A&AS 114, 393
Harmanec P., 1988 Bull. Astron. Inst. Czechosl. 39, 329
Harper W.E., 1937 Publ. Dominion Astrophys. Obs. Victoria 7, 1
Hauck B. 1986, A&A 154, 349
Henroteau F. 1919, Popular Astronomy 27, 29
Henroteau F. 1923, Publ. Obs. Univ. Michigan 3, 53
Hubeny I., Lanz T., Jeffery C.S. 1994, in Newsletter on Analysis of Astronomical Spectra No.20, C.S.Jeffery ed., St. Andrews University, p.30
Iliev I.K., Barzova I.S. 1994, in Chemically Peculiar and Magnetic Stars, J.Zverko & J.Žižňovský eds., Astron. Inst. Slovak Acad. Sci., Tatranská Lomnica, p.95
Jaschek C., Conde H., de Sierra A.C. 1964, Obs. Astr. Univ. Nac. La Plata, Ser. Astr. 28 (2), 1
Jerzykiewicz M. 1974, PASP 86, 675 and priv.comm.
Johnson H.L., Mitchell, Iriarte B., Wiśniewski W.Z. 1966, Comm. Lunar Planet. Obs. 4, 99
Kurucz R.L. 1993, Solar Abundance Model Atmospheres, Kurucz CD-ROM No.19
Lee O.J. 1908, Science 28, 853
Lloyd C. 1981, MNRAS 195, 805
Mayer P., Drechsel H. 1987, A&A 183, 61
McAlister H.A., Hartkopf W.I., Sowell J.R., Dombrowski E.G. 1989, AJ 97, 510
McAlister H.A., Hartkopf W.I., Franz O.G. 1990, AJ 99, 965
McAlister H.A., Mason B.D., Hartkopf W.I., Shara M.M. 1993, AJ 106, 1639
Moore C.E., 1945 A Multiplet Table of Astrophysical Interest, Contr. Princeton Univ. Obs. No. 20
Renson P., Faraggiana R., Boehm C. 1990, Bull. Inform. CDS, 38, 137
Smith M.A., 1985 ApJ 297, 206
Stellingwerf R.F. 1978, ApJ 224, 953
Stürenburg S. 1993, A&A 277, 139
Tarasov A.E., Harmanec P., Horn J., Lyubimkov L.S., Rostopchin S.I., Koubský P., Blake C., Kostunin V.V., Walker G.A.H., Yang S. 1995, A&AS 110, 59

© European Southern Observatory • Provided by the NASA Astrophysics Data System